Bulletin of the Seismological Society of America, Vol. 95, No. 1, pp. 277–293, February 2005, doi: 10.1785/0120030179

An Alternative Approach to the SPAC Analysis of Microtremors: Exploiting Stationarity of Noise

by Francisco J. Chávez-García, Miguel Rodríguez, and William R. Stephenson

Abstract The SPAC (Spatial autocorrelation) method to analyze ambient vibration records was introduced by Aki (1957). Currently, this method is being used for the analysis of microtremor data from an array of stations: crosscorrelation functions are computed between pairs of stations, and then averaged for different station pairs, at the same interstation distance but with different orientation. In this article we propose the idea of exploiting recordings of microtremors over long times as a substitute for spatial averaging, as was suggested in Aki (1957). This idea has several advantages. The two most important are, first, that it is not required to obtain simultaneous recordings using an array of stations, whose locations must obey a very rigid scheme; and second, the ability to obtain results for a large number of closely-spaced distance intervals. Our proposal is tested using data from the Parkway, Wainuiomata, temporary array. These data are supplemented with additional measurements performed during February 2003, to resolve an uncertainty regarding the low-frequency part of our results. Given the irregular distribution of our array, we are able to obtain results for many different station pairs. The phase-velocity dispersion curves we derive from our measurements, interpreted with the SPAC method, are compared with previous results in this sedimentary basin. Our results suggest that the SPAC method is more general than appears in recently published papers.

Introduction

Site effects play a major role in destructive ground motion. The effects of local geology may modify in a very significant way ground motion on soft soils, the case of the Mexico City earthquakes during 1985 being a foremost example. Ground motion was amplified by a factor of about 40 at the resonant frequency of the very soft soil layer covering the ancient lake bed zone. Site effects may be taken into account with relative ease when abundant records of ground motion exist for nearby stations on different soil conditions using, for example, spectral ratios (Chávez-García *et al.*, 1990). Usually, however, we must have recourse to exploration techniques to determine the subsoil structure and deduce from it the expected amplification.

More than 40 years ago, Aki (1957, 1965) proposed an innovative technique (the spatial autocorrelation, or SPAC, method) which used ambient vibration measurements to determine the underlying subsoil structure. Assume that we record microtremors using an array of stations on the free surface, and that we compute the crosscorrelation function between different pairs of stations, at the same interstation distance, sampling different orientations on the free surface. At this point, we require two hypotheses: (1) ambient vibration is stationary in both time and space, and (2) the wavefield consists of dispersive waves propagating along the free surface. Under these hypotheses, Aki (1957) showed that the ratio of the average of those different crosscorrelation functions and the autocorrelation function at a reference station (defined by him as the correlation coefficient) takes the form of a zero-order, first-kind Bessel function. In the argument of that Bessel function appear the fixed interstation distance, the frequency, and the phase velocity of the propagating waves. It is then possible to obtain a phase velocity dispersion curve using the records filtered in a series of narrow frequency bands. In recent applications of the SPAC method (Ferrazzini *et al.*, 1991; Metaxian, 1994; Chouet *et al.*, 1998), the seismographs have been disposed on half a circle, with a central station recording simultaneously. This array satisfies a requirement of the method, as it allows the sampling of different azimuths between pairs of stations at the same distance to compute the azimuthal average.

The original paper by Aki was based on data from two analog seismographs. Today, most studies use at least ten autonomous seismographs (Chávez-García *et al.*, 1999; Scherbaum *et al.*, 1999; Kanno *et al.*, 2000). However, the number of available instruments has not had any impact on the field procedure used to make measurements with the SPAC method. The stations continue to be placed forming a circle (Kanno *et al.*, 2000) or a semi-circle (Chouet *et al.*,

1998). An interesting extension of the method was presented in Asten (1976). This author showed that microtremors consisted of Rayleigh waves, and then proceeded to extend the SPAC method to include the possibility of the presence of different modes in the microtremor records. This allowed him to better constrain the geological model deduced from the SPAC measurements (Asten, 1978). However, the analysis of the data continued to follow the guidelines posed by Aki (1957).

In this article we have taken advantage of available ambient vibration records from a dense temporary digital seismograph network. The purpose of its installation was to better understand the relation between local geology and recorded ground motion in a small alluvial basin. As part of its operation, and for calibration purposes, the instruments of the network were triggered periodically and ambient vibration was recorded simultaneously. We have analyzed these data using the SPAC method. However, given that the installation of the network was guided by considerations such as security of the instruments during the two-month experiment, the spatial distribution of the array is very far from the ideal geometry for the SPAC analysis (concentric circles with stations covering all azimuths regularly). For this reason, in order to use the SPAC method with our data, we need to substitute temporal stationarity for spatial stationarity, an idea that was mentioned in Aki (1957). Our hypothesis is that, given long enough records of ambient vibration, the average spatial crosscorrelation between any given pair of stations is an adequate estimate of the azimuthal average of the same crosscorrelation functions. Aki (1957) observed that crosscorrelation along different directions did not differ significantly, concluding that "we may regard the microtremor as being propagated in every direction, each with almost uniform power". If microtremors propagate homogeneously in all directions, measurements along a single direction are equivalent to an azimuthal average. This hypothesis will have to be verified for our data.

In the next paragraphs we will first recall the main equations and the hypotheses behind SPAC. We will then discuss in detail the results obtained using the microtremor measurements recorded in 1995. We will discuss the limitations in the results that forced us to make a second campaign of measurements during February 2003. The results presented here show that it is possible to use the SPAC method with different array configurations, thereby expanding greatly the range of its application.

The SPAC Method

The measurement of the propagation velocity of seismic waves is a problem that occurs often in seismology. Starting from the pioneering work with the Lasa array in the 1960s (Capon, 1968; Lacoss *et al.*, 1969; Aki and Richards, 1980), it became clear that detection of seismic waves in the presence of noise and the measurement of its propagation velocity can be greatly enhanced using arrays of stations. This, of course, requires the hypothesis that the seismic wavefield that is seen by each element of the array is common to all stations—that is, the wavefield is homogeneous under all the spatial extent of the array. The number, type, and spatial arrangement of the sensors in the field, however, form a spatial filter through which the signals are filtered. Different methods have been devised to process data from arrays (either in passive or active seismology) in order to recover apparent velocity of the waves that cross it, (Toksoz, 1964). The high resolution *f–k* (frequency–wavenumber) method was introduced by Capon (1969) and, since then, has been extensively used. When a seismic source is used, group and/or phase velocity of surface waves can be measured using methods such as the multiple filtering technique (Dziewonski *et al.*, 1969; Herrmann, 1973), stacking (McMechan and Yedlin, 1981; Barker, 1988), or Spectral Analysis of Surface Waves (SASW) (Nazarian and Stokoe, 1984).

The SPAC (SPatial AutoCorrelation) method was first introduced by Aki (1957) to determine phase velocity using records of ambient vibration. Its theory was thoroughly developed in Aki (1957), where many different cases were treated (from a single, non-dispersive wave propagating with constant direction to the possibility of multiple dispersive, polarized waves propagating in all directions). Additional refinements of the method, as well as discussion of practical procedures, were presented in Aki (1965). The essence of the method is that, when we have records from seismic stations, spaced at a constant distance and forming pairs of stations along different azimuths, it is possible to compute an estimate of the phase velocity of the waves crossing the array, without regard to the direction of propagation of the waves present. The method assumes that the 2D wavefield being recorded by an array of stations is stochastic and stationary ambient vibration, in both space and time.

Let us consider a stochastic wavefield formed by the superposition of many plane waves propagating in many directions in the horizontal plane, non-polarized, and all of them propagating with the same constant phase velocity c. The ground motion at two locations on the surface, (x, y) and $(x + \xi, y + \eta)$, can be written as $u(x,y,t)$ and $u(x + \xi, y + \eta, t)$. The spatial autocorrelation function $\phi(\xi,\eta,t)$ is defined as

$$\phi(\xi,\eta,t) = \overline{u(x,y,t)u(x+\xi,\ y+\eta,t)}, \qquad (1)$$

where the bar indicates time averaging. Under the assumption that the wavefield is stationary, Aki (1957) showed that the azimthal average of the spatial autocorrelation function (Aki, 1957, equation 37) can be written as

$$\bar{\phi}(r) = \frac{1}{2\pi}\int \phi(r,\psi)d\psi, \qquad (2)$$

where r and ψ are the polar coordinates defined by

$$\xi = r\cos\psi$$

and

$$\eta = r\sin\psi.$$

Aki (1957) showed that the azimuthal average of the spatial autocorrelation function, $\bar{\phi}(r)$, and the power spectral density of the wavefield u, $\Phi(\omega)$, where ω is angular frequency, can be written as follows (Aki, 1957 equation 39):

$$\bar{\phi}(r) = \frac{1}{\pi}\int_0^\infty \Phi(\omega) J_0\left(\frac{\omega}{c}\, r\right) d\omega, \tag{3}$$

where J_0 is the Bessel function of first kind and zero order. Note that the argument of the Bessel function may be also written as

$$\frac{\omega}{c}\, r = kr = \frac{2\pi r}{\lambda},$$

where k is the wavenumber and λ is the wavelength. Equation (3) also applies to the case of dispersive waves, as shown in Aki (1957). We need only substitute $c(\omega)$ for c. Consider now that we apply a bandpass filter to the signals. The spectral density becomes

$$\Phi(\omega) = P(\omega_0)\delta(\omega - \omega_0), \tag{4}$$

where $P(\omega_0)$ is the power spectral density at frequency ω_0 and $\delta()$ is Dirac's function. In this case, the azimuthal average of the spatial correlation function (Aki, 1957 equation 41) can be written as

$$\bar{\phi}(r) \equiv \bar{\phi}(r,\omega_0) = P(\omega_0) J_0\left(\frac{\omega_0}{c(\omega_0)}\, r\right). \tag{5}$$

Now, let us define the autocorrelation coefficient (Aki, 1957) as

$$\rho(r,\omega_0) = \frac{\phi(r,\psi,\omega_0)}{\phi(0,\psi,\omega_0)}. \tag{6}$$

As $P(\omega_0)$ does not depend on the position, then we can write the azimuthal average of the spatial correlation coefficient finally as

$$\rho(r,\omega_0) = J_0\left(\frac{\omega_0}{c(\omega_0)}\, r\right). \tag{7}$$

The preceding derivation was presented in great detail in Aki (1957) and also in Metaxian (1994) and Chouet *et al.* (1998), among others. The last equation offers a way to compute the phase velocity, when we can estimate an azimuthal average of the spatial autocorrelation, for a fixed distance r. This was interpreted, starting with Aki (1965), as requiring several stations, distributed on a circle of radius r, with one station at the center of the circle. Naturally, if data recorded on several circles with different radii are available, an azimuthal average can be computed for each circle, and for a fixed frequency ω_0, using r as independent variable.

The SPAC method, and its extension to the case of polarized waves also discussed in Aki (1957), has been applied at many different sites to determine an average shear-wave velocity profile under the installed array (Ferrazzini *et al.*, 1991; Metaxian, 1994; Chouet *et al.*, 1998; Yamamoto, 1998; Morikawa *et al.*, 1998). Aki (1957, p. 431) showed that, when the measured wavefield is isotropic, (i.e., its spatial spectral density depends only on the horizontal wavenumber, but not on the direction), $\bar{\phi}(r)$ (the azimuthal average of the spatial autocorrelation function) can be replaced by $\phi(r,\psi)$ (the spatial autocorrelation function for an arbitrary ψ). This was subsequently proved by Asten (1976) in the frequency domain. He assumed that ambient vibration, at a given frequency ω_0, consists of a large number of plane waves distributed uniformly in azimuth, that is, isotropic, and distributed over wavenumber with power density $p(k)$, so that $\int_0^\infty p(k)dk = 1$. He showed that the coherency between an arbitrary pair of stations recording this ground motion can be written as:

$$C(\omega,r) = \delta(\omega - \omega_0)\int_{k=0}^{\infty} J_0(kr)p(k)dk, \tag{8}$$

where $C(\omega,r)$ is the coherency between two stations separated a distance r, and k is the wavenumber. If wave propagation is restricted to a single scalar wavenumber k_0, then

$$C(\omega,r) = \delta(\omega - \omega_0)J_0(k_0 r). \tag{9}$$

Under the assumptions we have made, equation (9) is the frequency domain version of equation (7). Thus, it is possible to use SPAC either in the time domain (through the crosscorrelation coefficient) or in the frequency domain (through the coherency). Using SPAC, the final product is a phase-velocity dispersion curve that corresponds to the subsoil structure, assumed to be the same below all the stations of the array. This dispersion curve can then be inverted to obtain a shear-wave velocity profile, using standard techniques (Herrmann, 1987).

Once we have an estimate of the correlation coefficients $\rho(r,\omega_0)$, we may use equation (7) as the basis for an inversion procedure to compute $c(\omega)$. We can state our problem as: determine the values of $c(\omega)$ that make the difference between our correlation coefficients and the function $J_0\left(\frac{\omega}{c(\omega)}\, r\right)$ the smallest. This is a non-linear problem for which

a linearizing transformation cannot be found. It can be written (using the standard notation in inversion texts) in matrix form as

$$d_0 = g(p), \tag{10}$$

where d_0 is the dataset, (i.e., our correlation coefficients for all distances and frequencies), p is the set of parameters we are inverting for, in our case, the values of the phase velocity for all frequencies, and $g()$ is the function that relates the observations with the parameters we are inverting for, in our case, it is the zero-order, first-kind Bessel function. Equation (10) is nothing more than the restatement of equation (7), describing the relation between the data we measure ($\rho(r,\omega_0)$) and the parameters we wish to obtain ($c(\omega_0)$), and assumes that our model (the J_0 function) represents without error the crosscorrelation coefficients as demonstrated by Aki (1957).

The procedure we have chosen is that proposed by Tarantola and Valette (1982) and later described in detail by Menke (1984). First, *a priori* values, p_0, for the parameters p are chosen. We have used a phase velocity dispersion curve of the form

$$c(f) = Af^{-B} \tag{11}$$

where f is the frequency, and A and B are constants. The choice of this function is not critical, provided that the initial guess is not too far from the final solution. By choosing this function, we express our expectation for the final shape of the phase-velocity dispersion curve. An interative procedure of solution is used where the initial guess of the value of parameters p at iteration step $k + 1$, p_{k+1}, is taken as the value estimated at iteration step k. The equation used to compute the updated values of p (Menke, 1984) is

$$p_{k+1} = p_0 + C_{p_0p_0} G_k^T (C_{d_0d_0} + G_k C_{p_0p_0} G_k^T)^{-1} [d_0 - g(p_k) + G_k(p_k - p_0)], \tag{12}$$

where p_k and p_{k+1} are the parameters that resulted from the inversion in steps k and $k + 1$ respectively, $C_{p_0p_0}$ is the covariance matrix of the parameters, $C_{d_0d_0}$ is the covariance matrix of the data, $g(p_k)$ is the Bessel function of zero order and first kind, evaluated with the parameters that resulted from the k^{th} iteration, and G_k is the matrix that contains the partial derivatives of the data (d_0) with respect to the parameters (p_k). The superindex T indicates the transposed matrix. Obviously, for the first iteration, $k = 0$ and the last term in equation (12) is equal to zero.

For our case, and given equation (7), the elements of matrix G_k take the form

$$\frac{\delta g(p)}{\delta c(\omega)} = \frac{\omega r}{c^2(\omega)} J_1\left(\frac{\omega r}{c(\omega)}\right). \tag{13}$$

In linear mechanics, the values of phase velocity at different frequencies are independent. However, this does not guarantee that the final dispersion curve will be smooth, as it is in nature. In order to obtain a final dispersion curve that is a smooth function of frequency, Tarantola and Valette (1982) suggested using the following expression as the covariance matrix of the parameters

$$C_{p_0p_0}(\omega,\omega_0) = \sigma^2 \exp\left[\frac{-1}{2}\frac{(\omega - \omega_0)^2}{\Delta^2}\right]. \tag{14}$$

This last expression indicates that the covariance matrix for the parameters of the model at frequency ω_0 is smoothed in frequency with a filter that depends on σ, the maximum accepted change of each parameter p between two iterations, and Δ, the width of the smoothing window in frequency. This filter assigns a larger weight to neighboring frequencies and a smaller weight to more distant frequencies. The use of this covariance matrix to weight the parameters of the model gives the most likely solution. Any other weighting gives a solution with a lower probability of being correct.

Our data are correlation coefficients computed from many different time windows. Thus, we are able to estimate, for each frequency and distance, an expected value plus a variance associated at that data point. Those variance values were used to build the covariance matrix of the data, $C_{d_0d_0}$.

Finally, consider the error estimates of the inversion procedure. The estimate we have used is again from Tarantola and Valette (1982). After the last iteration, the *a posteriori* covariance matrix of the parameters p is computed as

$$C_{pp} = C_{p_0p_0} - C_{p_0p_0} G^T (C_{d_0d_0} + G C_{p_0p_0} G^T)^{-1} G C_{p_0p_0}. \tag{15}$$

An additional problem that is not often discussed is the range of validity of the results from the SPAC method. This range was computed by Henstridge (1979) as going from 0 to 3.8 units of the argument of the Bessel function inverted from the coefficients. In that article, Henstridge (1979) discusses why that range cannot be used in its entirety. The reason is that the variance associated with the estimate of the phase velocity from the correlation coefficients can be written as follows (Henstridge, 1979):

$$Variance[\tilde{k}(\omega)] \approx Variance[\rho(r,\omega)] \left\{ rJ_1[rk(\omega)] \right\}^{-2}, \tag{16}$$

where $k(\omega)$ is the wavenumber at frequency ω, $\tilde{k}(\omega)$ is its estimate, r is the interstation distance, and J_1 is the first-order Bessel function of the first kind. According to this equation, the estimate of the wavenumber, $\tilde{k}(\omega)$, has a variance that is inversely proportional to the square of J_1. This latter function is zero when its argument is 0 and when it is 3.8. At these values of the argument, the estimate of the wavenumber,

$\tilde{k}(\omega)$, has an error that increases without bound. Henstridge (1979) suggests considering the results valid only when the argument of the Bessel function is between 0.4 and 3.2. These values imply that the estimate of $k(\omega)$ will be valid in the range $2 < \lambda/r < 15.7$. If we consider as an upper limit for the argument the value 3.8, then $\lambda/r > 1.7$. These are the values currently referred to in the literature, and thus, the limits of validity established by Henstridge continue to apply. We will discuss later the way in which these limits apply to our data.

We observe, then, that the restriction to a circular array does not appear in the original paper (Aki, 1957). Moreover, the data used in that paper corresponded to station pairs analysed independently. Other authors have used versions of the method that do not require a strict circular geometry in the array. Bettig *et al.* (2001) presented a small modification of circular based SPAC. They computed the corrections needed by the method, when the stations are off the perfect circular geometry. Those corrections allow the use of SPAC when constraints in the field imposed small modifications to the perfectly circular geometry. A bolder approach is that of DeLuca *et al.* (1997), who used recorders arranged along a line, installed with the purpose of recording an explosion. However, DeLuca *et al.* (1997) do not justify why SPAC would be valid for the geometry of their array, nor do they include any detail of their computations (e.g., how are average correlation coefficients computed). The paper by Ohori *et al.* (2002) is more complete. They present a derivation of the method that follows closely that of Asten (1976), and arrive at our equation (9) (their equation 3). In that derivation they clearly state that an azimuthal average is required; otherwise it not possible to obtain the Bessel function. However, when they apply the method to the data from their two T-shaped arrays, they neglect to explain how do they avoid the requirement to have an azimuthal average.

In this article we have used the SPAC method, as described. We analyze only the vertical component. The only change we introduce is that we do not apply an azimuthal averaging to the correlation coefficients. We make the hypotheses that the ambient vibration wavefield is ergodic and isotropic. Under these assumptions, the wavefield includes propagation in all directions with similar power, and may be observed using a single, arbitrarily oriented pair of stations. In the next sections we demonstrate the validity of these hypotheses for our data, something that was neglected in previous studies using SPAC with a non-circular array.

Data of the 1995 Experiment

The field experiment where the data was recorded has been described in previous articles (Chávez-García *et al.*, 1999, 2002). We will recall only the most important points. A temporary network of 24 digital seismographs was installed from 1 August until 12 October 1995, in Parkway valley, Wainuiomata, New Zealand. Each station consisted of a 1-Hz, three-component seismometer coupled to an EARSS (Equipment for the Automatic Recording of Seismic Signals) seismograph (Gledhill *et al.*, 1991). Time was received by each station from the official time broadcast in New Zealand. Station P01 was installed about 2 km to the northeast of the basin, on firm rock. Four of the remainder stations were installed on the soft rock (weathered greywacke) surrounding and underlying Parkway basin, while 19 others were installed on the soft sediments filling the valley. A description of the local geology around Parkway has been given in Chávez-García *et al.* (1999). The average distance between neighboring stations was 40 m. Figure 1 shows the distribution of the stations, with the exception of station P01, outside the area mapped.

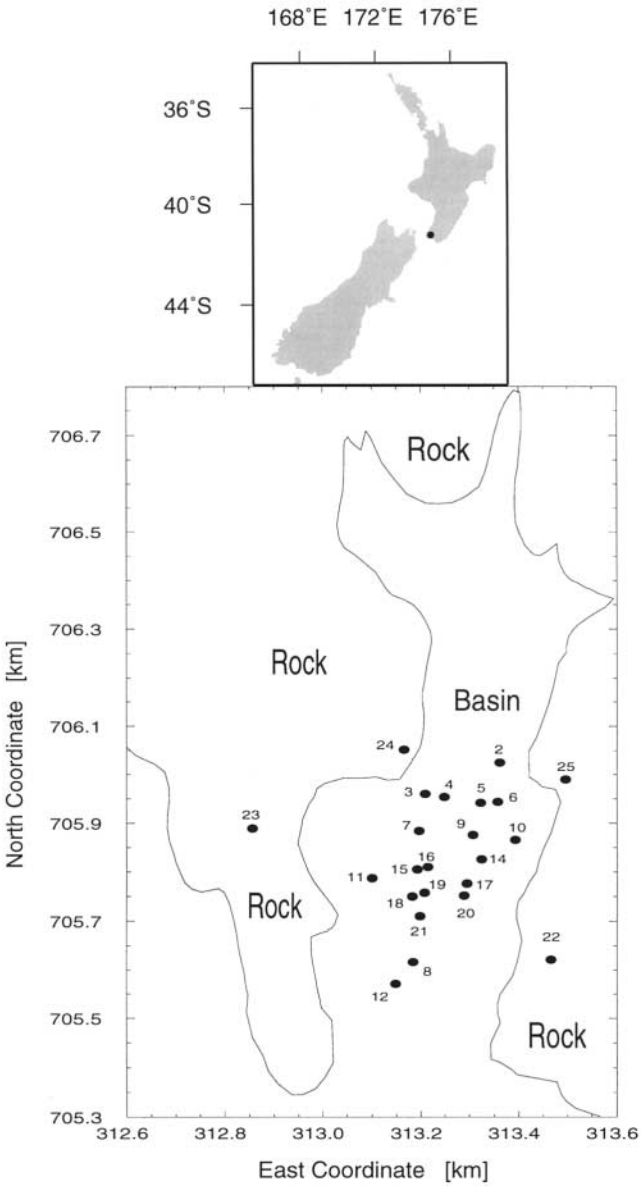

Figure 1. Location map and distribution of the stations in Parkway valley, Wainuiomata, New Zealand. The thin line shows the limits between soft soil sediments and underlying rock.

The main purpose of the network was to record earthquakes. However, as part of its operation, the network was programmed to trigger periodically to verify its status. Thus, one-minute time windows of ambient vibration were recorded simultaneously by the stations every hour for each day the network operated. This system generated a very large amount of microtremor data. Clearly, however, the spatial distribution of stations shown in Figure 1 is far from the concentric circles required by the SPAC method. However the distances between stations on the soft sediments sample in detail the distance range between 22.8 m (distance between stations 15 and 16) and 501 m (distance between stations 02 and 12). We have not used all microtremor records obtained from the network during its more than 2-month operation. Rather, we selected three different days and used the 24 one-minute windows recorded by each station each day. At this stage we considered only vertical motion. Due to some malfunctions, not all stations recorded the 72 microtremor windows. The average number of windows for all station pairs was 63.

Results Using the Data from the 1995 Experiment

Before going on to apply SPAC to our dataset, we need to show that our hypothesis of isotropic propagation (similar power propagating in all directions) holds. To this end, we have computed *f–k* spectra using sample ambient vibration records. We have chosen four 60-sec windows of ambient vibration, and computed high resolution *f–k* spectra (Capon, 1969). Before this computation, the traces were bandpass filtered in a series of 0.4-Hz-wide frequency bands, with a 0.2 Hz overlap between neighboring windows. The filter used was a four pole, zero-phase Butterworth filter. The results are shown in Figure 2. The determined backazimuths (Fig. 2a) are extremely variable for each of the four windows analyzed. There is no single direction from which energy arrives in a coherent way. This means that ambient vibration results from the contribution of many different sources at many different locations, and that the subsoil structure does not favor a particular direction of propagation. Figure 2a demonstrates the hypothesis that the energy is propagating in almost all directions with similar power (i.e., the wavefield is isotropic). Figure 2b shows the phase velocities determined. Clearly, *f–k* spectra are able to indicate that most of the energy travels with low phase velocity, but the results are marred both by aliasing problems and by the inability of f–k spectra to determine a phase velocity when many signals are present in the records with similar power.

We have now computed crosscorrelation coefficients using each pair of stations. The computations are straightforward. We considered the 63 (on average) one-minute microtremor records for each station. When there were simultaneous records at any pair of stations, we filtered the traces using a series of 30 bandpass filters, 0.5 Hz wide, centered at frequencies between 0.75 Hz and 8 Hz, with a 0.25-Hz frequency step. The filters used were Butterworth, 8 pole,

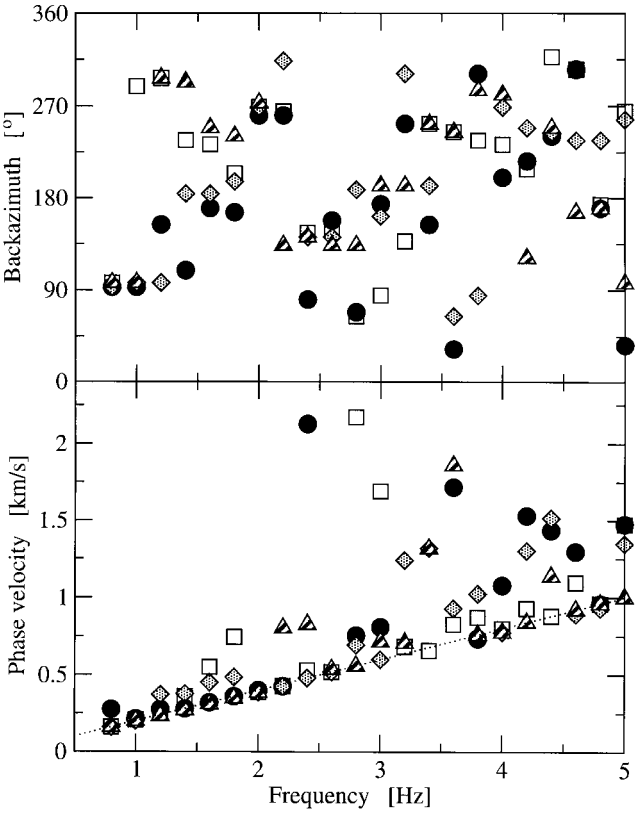

Figure 2. Results of *f–k* analysis for a sample of four 60-sec windows of ambient vibration recorded by the stations on sediments during the 1995 experiment. Each different symbol corresponds to a different time window of analysis. An *f–k* spectrum was computed for a series of window frequencies, 0.4-Hz wide. The corresponding symbol is plotted at the central frequency of each window. (a) Backazimuth. (b) Phase velocity. The dotted line in panel (b) is the line of constant wavelength for a wavenumber of 5 cycles/km, the maximum value for which the *f–k* spectra were computed.

zero-phase. We repeated the computation using different filters, and the results were always very similar. Each pair of filtered traces was multiplied (corresponding to the spatial crosscorrelation between those traces for a single distance-delay). The time average of the resulting trace, normalized by time average of the square of any one of the two traces, is the correlation coefficient for that frequency and that distance, according to the definition by Aki (1957). Finally, we averaged the crosscorrelation coefficients as a function of frequency, for all time windows common to a given station pair. If we consider that the ambient vibration is a random variable with normal distribution (as is usually accepted), the probability distribution of the crosscorrelation coefficients will be that of a product of two random variables with normal distribution, (i.e., not the normal distribution). However, we averaged many estimates of the correlation coefficients, as many as the number of time windows we use. For this reason, taking recourse to the central limit theorem (Pa-

poulis, 1984), it does not matter what the probability distribution function of the correlation coefficients is. We can assume that the probability distribution of the average crosscorrelation coefficients is Gaussian.

For some station pairs, the crosscorrelation coefficients at the lowest frequency (0.75 Hz) were low (<0.75). Those crosscorrelation coefficients were discarded because they contradict the fundamental hypothesis that the recorded microtremor wavefield is common to the stations. A set of crosscorrelation coefficients that does not tend to unity at low values of the argument indicates that the two stations involved are affected by different sources of ambient vibration. This was verified when, going back to the time signals, we observed transients at one station that were not recorded at the second one. Small crosscorrelation values at low frequencies were consistently observed for correlations computed between a station on soft soil and a station on rock. This was to be expected. Indeed, if microtremors consist of Rayleigh waves, they are guided by the layered structure beneath the station. This structure may be similar for two stations on soft soil, or for two stations on rock, but it will be different for two stations, one on soil and one on rock. In addition, for most of the pairs of stations on rock, crosscorrelations were low and the results were inconsistent with those for the soft soil stations, and we were forced to discard them. The final selection of results led us to keep 70 station pairs (all of them on soft soil) with inter-station distance ranging from 40 to 396 m. In contrast, many studies using SPAC (Morikawa *et al.*, 1998) usually report crosscorrelation coefficients for only 2 different distances. Figure 3a shows the average crosscorrelation coefficients as a function of frequency and distance. For the purpose of this figure only, we linearly interpolated the correlation coefficients with distance. The solid diamonds in Figure 3a indicate the frequency at which the average goes through zero, as a function of distance. We observe that the frequency of first-zero-crossing of the crosscorrelation coefficients shifts to lower values with increasing distance between stations. This is what we anticipated, because we expect that crosscorrelation between two stations will have large values only for frequencies for which the corresponding wavelength is large compared with the inter-station distance. Thus, smaller inter-station distances contribute information in the higher-frequency range, while the larger distances constrain the dispersion curve at lower frequencies. Figure 3a shows the steady decrease in frequency of the first zero crossing with increasing distance. We also observe that for distances larger than 210 m this value remains approximately constant. For the argument of the Bessel function ($\omega r/c$) to remain constant, any increase in r must be matched by a proportional increase in c; the phase velocity estimated from larger inter-station distances will have larger values. The constancy of the frequency of the first zero crossing with increasing distance can also be interpreted in terms of site response. When the frequency at which our data has its useful information (around the first zero of the Bessel function, which is obtained for any pair of stations separated a distance equal to one fourth of the wavelength) coincides with the frequency of resonance of the sediments, correlation persists independent of distance increases. For frequencies lower than the resonant frequency (at Parkway it is between 1.5 and 1.7 Hz), the surface waves should go into the basement. However, if the impedance contrast is large (as in Parkway), the microtremor energy in the sediments remains trapped in the sediments, and our measurements do not carry information on shear-wave velocities below the sediments; therefore, the frequency of the first zero crossing does not decrease further.

Figure 3b shows the coefficient of variation of the crosscorrelation coefficients (standard deviation divided by mean value), again as a function of frequency and distance. For the purpose of this figure only, the coefficient of variation was linearly interpolated with distance. For low values of frequency, the mean value is larger than the standard deviation, indicating that the result is statistically significant. The open diamonds in this figure indicate the frequency at which the coefficient of variation takes the value of unity. For each distance, the better results are those for frequencies smaller than that of the corresponding diamond. The location of diamonds in Figure 3b mimics that in Figure 3a, indicating that only the frequency range around the first zero crossing of the crosscorrelation coefficients contributes significant information.

Equation (7) shows that we can consider the correlation coefficients for a fixed distance, and obtain the Bessel function. In a similar way, as proposed in Ohori *et al.* (2002), we can fix the frequency and consider the variation of the crosscorrelation coefficients as a function of distance. That both positions are appropriate is shown in Figure 4, where we have plotted the correlation coefficients as functions of distance for four chosen values of the frequency. At 1 Hz, the correlation coefficients do not go through zero, indicating that we should have larger inter-station distances to obtain useful information at this frequency. At 1.5 Hz, the first zero crossing occurs at a distance of about 300 m; at 100 m at 2.25 Hz; and at 50 m at 3.25 Hz.

At this point, we can verify two of the hypotheses we have assumed in this article. The first one is that we can model the records of ambient vibration as an ergodic, stochastic process. This can be shown by comparing the estimates of the crosscorrelation coefficients among all the individual time windows used to compute its average value. This is shown in Figure 5, for a sample of four different inter-station distances. Each solid line in this figure corresponds to the crosscorrelation coefficients estimated from a single, simultaneous, one-minute-duration microtremor recording at a pair of stations separated by the distance indicated in each panel of this figure. The open circles are the average values, each of them including an estimate of the standard deviation. We observe that our hypothesis is backed by our data. Again, the results at smaller inter-station distances are stable over a larger frequency range. As the inter-station distance increases, the average value becomes con-

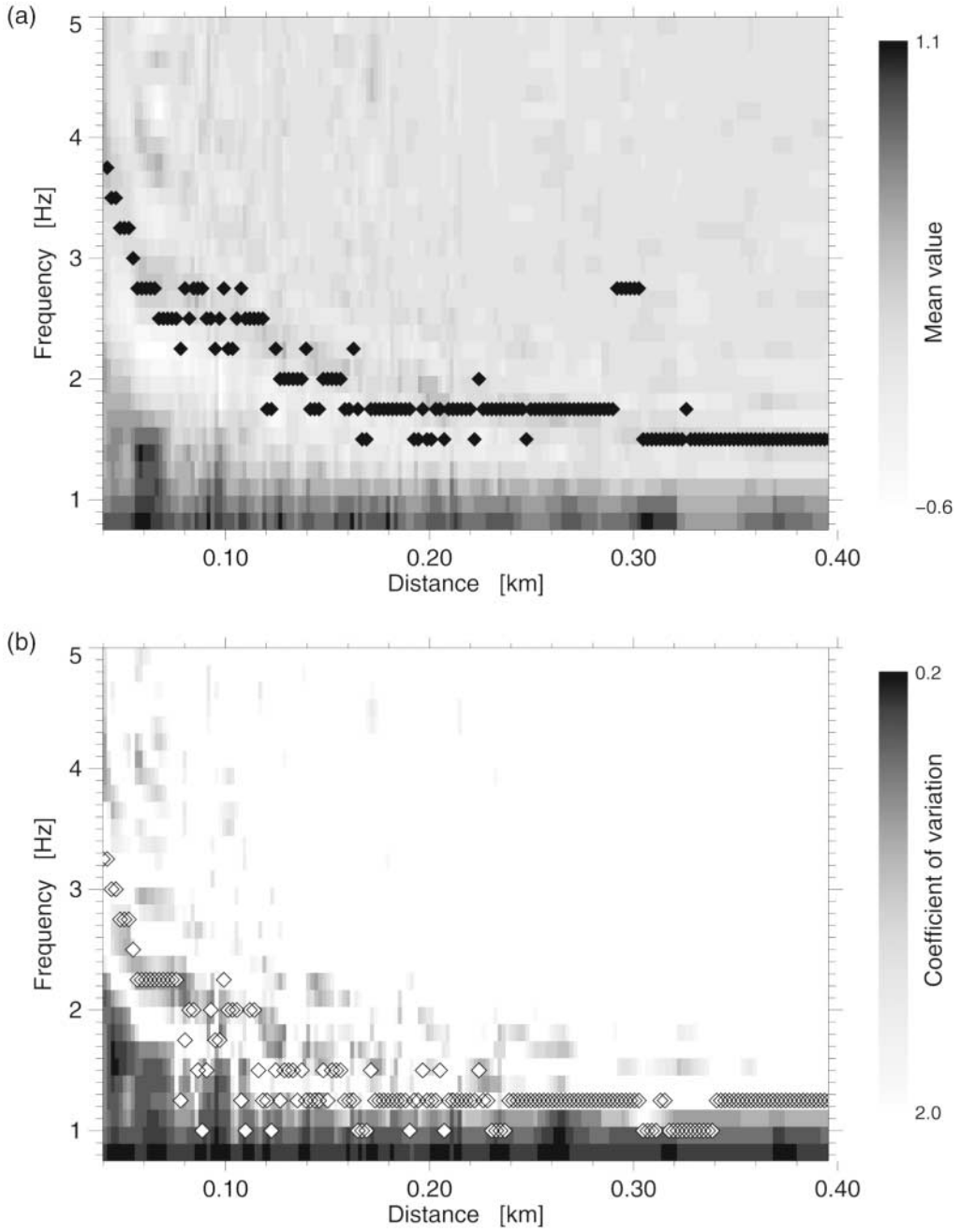

Figure 3. (a) Average value of the crosscorrelation coefficients as a function of frequency and distance. The solid diamonds indicate, for each distance, the frequency at which the correlation coefficient first goes through zero. (b) Coefficient of variation (standard deviation divided by the mean value) of the correlation coefficients as a function of frequency and distance. The open diamonds indicate, for each distance, the frequency at which the coefficient of variation takes the value of unity. All station pairs on soft soil in Parkway basin for the 1995 experiment were used. For the purpose of this figure only, correlation coefficients were linearly interpolated with distance.

stant at smaller frequency values (4 Hz for 138 m; 3.5 Hz for 214 m; and 2.5 Hz for 396 m), and the scatter of the individual estimates becomes larger than the average values.

Consider now the validity of substituting the azimuthal average for the time average between a single pair of stations for many time windows. Our array is not circular; however, we have selected 4 stations (09, 14, 11, and 21) that are at approximately the same distance from station 16 (113 m at station 09; 117 m at station 11; 111 m at station 14; and 101 m at station 21). These 4 stations are located on two of the

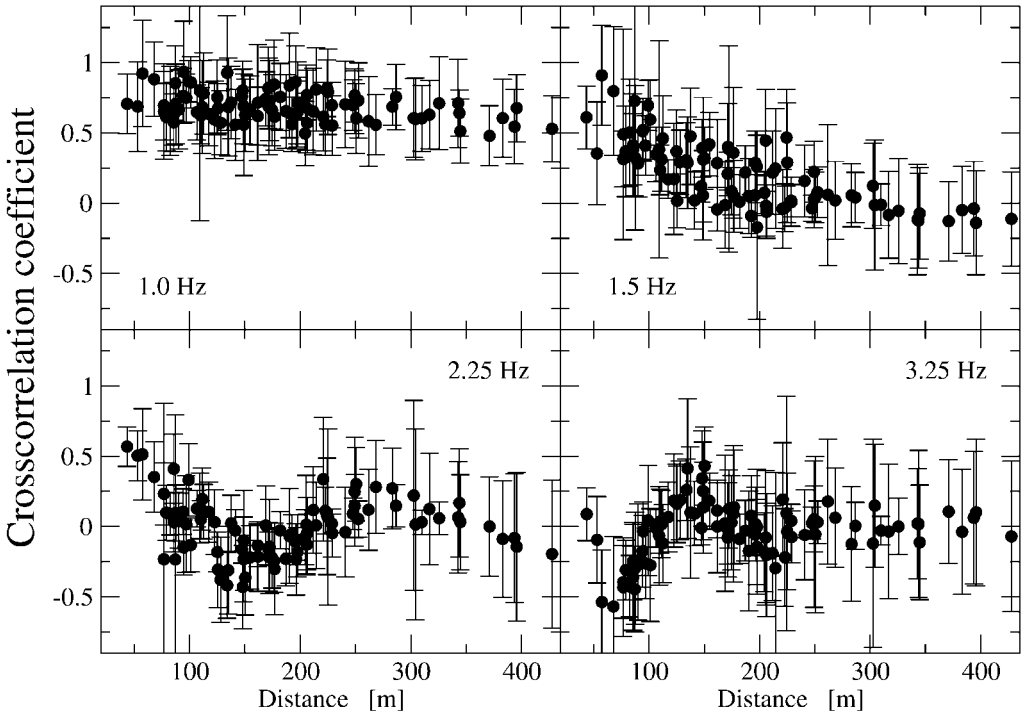

Figure 4. Crosscorrelation coefficients as a function of distance for four different values of frequency. Each solid circle shows the mean value at a given inter-station distance. The vertical bar at each symbol indicates the standard deviation computed for all time windows analyzed for each pair of stations, assuming normal distribution.

four quadrants from station 16. Each solid line in Figure 6 shows the azimuthal average for a single one-minute window of measurements computed as the average of the correlation between station 16 and each of stations 09, 14, 11, and 21. Each of those lines, then correspond to an estimate using the classical SPAC approach. The open circles in Figure 6 show the average crosscorrelation estimated using only data from the station pair 16–09 (71 one-minute windows). Each open circle is drawn with its associated standard deviation. We observe that the long term average between a single station pair closely represents the azimuthal average for a given inter-station distance.

Once we had estimates of the correlation coefficients as a function of frequency and distance, we inverted them to obtain the phase velocity dispersion curve, $c(\omega)$. The procedure outlined previously, minimizing the difference between $\rho(r,\omega_0)$ and $J_0\,(\omega_0/c(\omega_0)r)$, was used. The values chosen for the *a priori* model parameters (equation 11) were $A = 1500$ and $B = -1$. These values generate an initial phase-velocity dispersion curve that is close to previous results in this basin (Chávez-García *et al.*, 2002). The constants chosen for the covariance matrix of the parameters (equation 14) were $\Delta = 0.4$ and $\sigma = 500$ m/sec. These values led us to an initial guess of the phase-velocity dispersion curve that was not very different from the final solution. In addition, we repeated the inversion many times using different values, and verified that the final results were very similar. Figure 7 shows an example of the results of these inversions for the two inter-station distances of 44 and 206 m. We observe that our average crosscorrelation coefficients have the shape of a zero-order, first-kind Bessel function, and that the estimated Bessel functions show a very close fit with the observations. Figure 7 shows clearly the difference between the abscissae at first zero crossing of the two functions plotted. The crosscorrelation coefficients for 44 m distance go through zero at 3.5 Hz, while those for 206 m go through zero at 1.5 Hz.

The inversion of the crosscorrelation coefficients at any one distance allows, in principle, the phase velocity dispersion curve to be obtained in the frequency range imposed by the criterion of Henstridge (1979). We have chosen instead to make a joint inversion of the whole set of crosscorrelation coefficients, simultaneously, for 71 different distances, using the procedure described in the previous paragraph. However, for each single distance, we included as data only those correlation coefficients satisfying Henstridge's (1979) criterion. The result is shown in Figure 8, obtained from the data shown in Figure 3. In that same figure we have superposed the lines corresponding to Henstridge's (1979) criterion for our two limiting distances: 40 and 396 m (the second line for $r_{\max}$ falls outside the plotted area). The results of the inversion are unreliable for wavelengths smaller than 80 m (twice 40 m, $r_{\min}$ the smaller spacing in our data). Between 1.5 Hz and 4 Hz we have a good coverage, while only two points of the dispersion curve could be computed for frequencies smaller than 1.5 Hz. The results shown in Figure

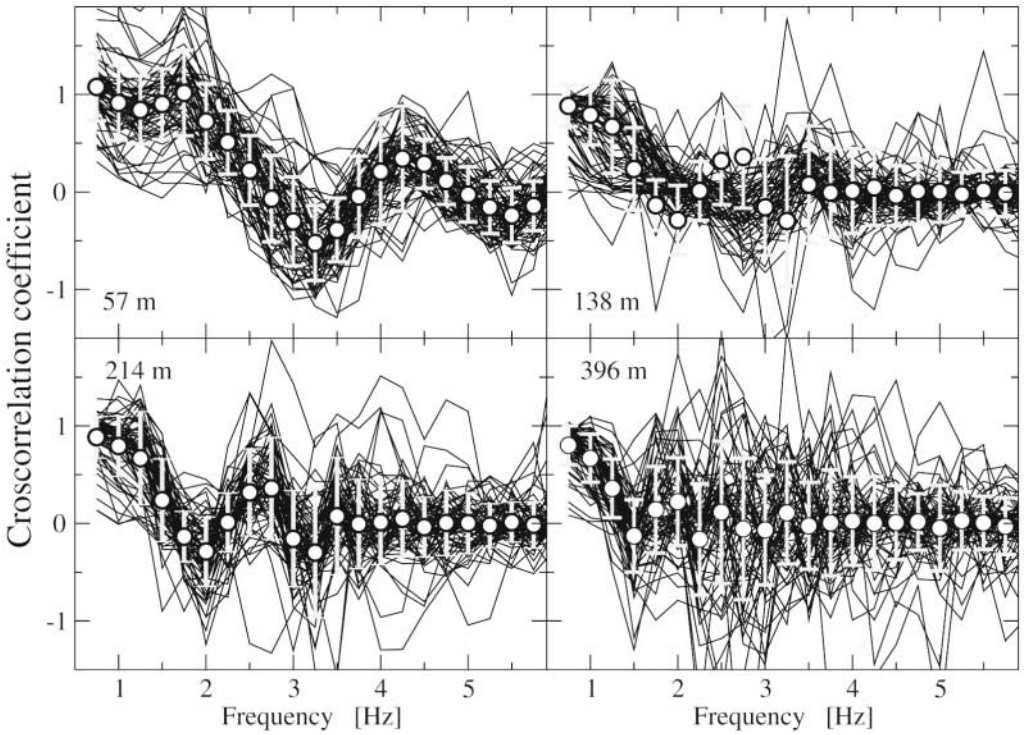

Figure 5. Crosscorrelation coefficients as a function of frequency for four different station pairs. Each solid line in each diagram corresponds to the crosscorrelation computed between a pair of stations for a single one-minute record of ambient vibration (70 windows for 57 m, 68 windows for 138 m, 68 windows for 214 m, and 70 windows for 396 m). The open circles and their associated error bars indicate the mean and standard deviation values computed at each frequency, assuming normal distribution.

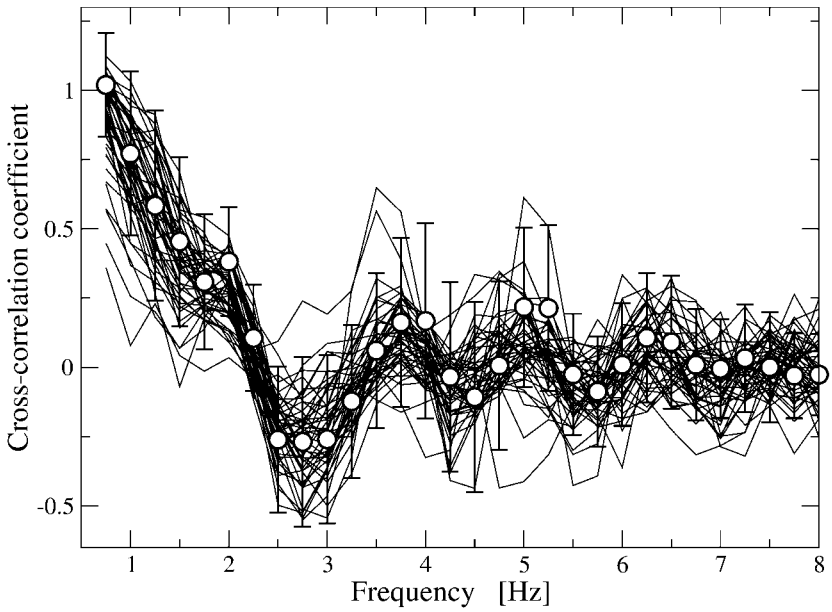

Figure 6. Comparison between correlation coefficients computed using azimuthal average with the results of using a single station pair. Each solid line shows the average of the correlation coefficients computed between stations 16–09 (separated 113 m), 16–11 (separated 117 m), 16–14 (separated 111 m), and 16–21 (separated 101 m) for a single, simultaneous, one-minute record of ambient vibration. This azimuthal average could be computed for 48 time windows. The open circles and their error bars show the average and the standard deviation (assuming normal distribution) of the correlation coefficient computed for 71 one-minute records of ambient vibration between stations 16 and 09.

8 indicate that we observe a single Rayleigh wave mode. Figure 8 also shows that we obtain no constraint on the phase velocity below the very soft sediments filling Parkway valley. In terms of ground motion, Figure 8 indicates that the Rayleigh waves we detect with SPAC are trapped within the sediments and convey little, if any, information on the underlying layers. The phase-velocity dispersion curve obtained using SPAC is compared in Figure 8 with the phase velocity obtained from the detailed *f–k* analysis of earthquake data recorded by Parkway array for the 10 best re-

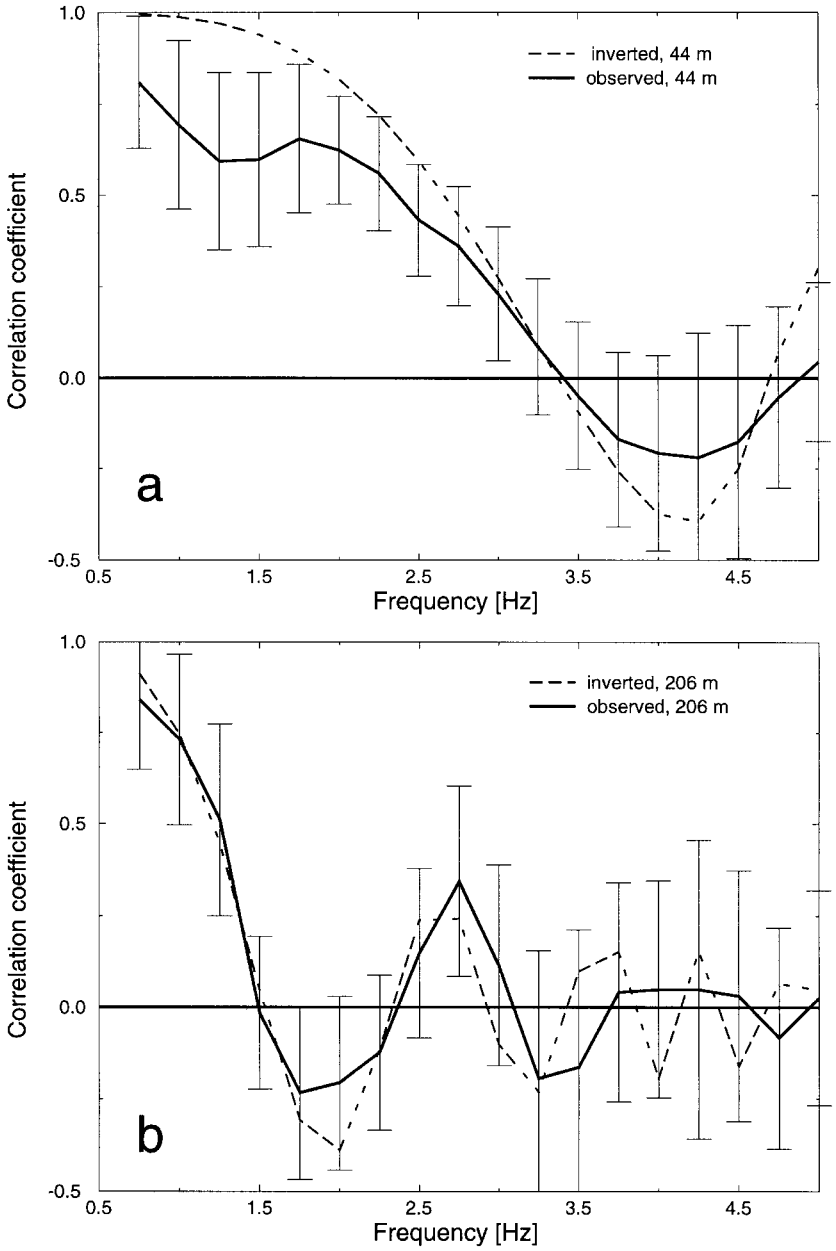

Figure 7. Example of the inversion of two crosscorrelation coefficients (solid lines) to obtain the corresponding Bessel function (dotted lines). Results are shown for two individual inter-station distances, 44 m and 206 m. Note the good fit between observations and the inverted Bessel function at its first zero crossing. This value controls the results.

corded events (open diamonds, Chávez-García *et al.*, 2002). The dot-dashed line shows the fundamental mode phase-velocity dispersion curve computed for the model established by Stephenson and Barker (2000) for Parkway basin using seismic CPT. The agreement is good for frequencies above 1.7 Hz, and poor for lower frequencies, supporting the idea that results from the SPAC method are not correct for frequencies lower than the resonant frequency in the basin. This is consistent with the idea that surface waves inside the valley are trapped in the sediments (because of their large impedance contrast with the basement) and convey little information of the underlying strata (Chávez-García *et al.*, 1999).

In order to obtain a phase velocity for the layers below the soft sediments filling Parkway valley, we computed the correlation between pairs of station on rock, P01, P22, P23, P24, and P25 (inter-station distances between 336 and 2230 m). However, the results were not useful. Results for three pairs of stations showed correlation coefficients that had the shape of a J_0 function, but the frequency of their first zero crossing was higher than that determined from soft soil stations for the same inter-station distance. Average correlation coefficients computed for the remaining seven pairs of stations were very close to zero for the whole frequency range considered (0.75–8 Hz). We can think of several reasons for this. Figure 1 shows that the assumption that the subsoil structure is the same does not hold for the rock stations, with Parkway valley in between. Another possibility is that there is some correlation in the ground motion between our rock stations, but it exists only for frequencies

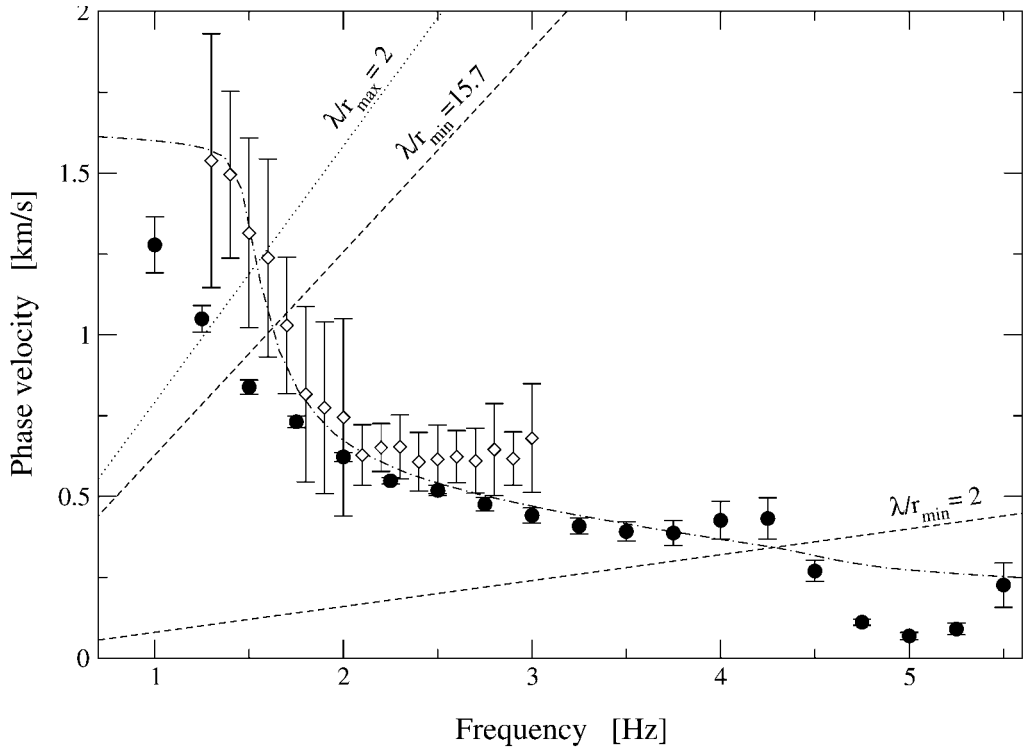

Figure 8. Solid circles indicate phase-velocity dispersion curve inverted from the data shown in Figure 3. The dotted and dashed lines show the limits imposed by Henstridge's (1979) criterion, computed for $r_{max} = 396$ m and $r_{min} = 40$ m. λ is the wavelength. The open diamonds show the phase velocity obtained from the detailed *f–k* analysis of earthquake data recorded by Parkway array for the 10 best recorded events (Chávez-García *et al.*, 2002). The dot-dashed line shows the fundamental mode phase-velocity dispersion curve computed for the model established by Stephenson and Barker (2000) for Parkway basin.

lower than the limit imposed in our measurements by the 1 Hz seismometers used in 1995. In order to explore this possibility, we decided to make an additional recording experiment, carried out during February 2003.

Data of the 2003 Experiment

Because part of the limitations observed during the analysis of the data recorded in 1995 may have come from the frequency response of the sensors, we decided to record for a one-week deployment using lower-frequency seismometers. The seismometers used were five Guralp CMG40 coupled to Orion recorders, from Nanometrics. These data loggers have 24-bit A/D converters and were synchronized using a GPS receiver at each station. We attempted to reuse as closely as possible the rock sites of the 1995 experiment. However, only P01 (renamed Rafter) and P24 (renamed Mo51) were exactly the same. The other sites were within 130 m from P22, P23, and P25, and could also very well have been selected in 1995. The map of the array used in 2003 is shown in Figure 9.

The stations were in place and continuously recording together for two full days. From this time period, we chose 126 one-minute-long simultaneous recording windows at all five stations. Once again, we analyzed only the vertical component. They were processed in the same way as the data from the 1995 experiment, with the exception that the lowest central frequency of the filters used was 0.3 Hz.

Results Using the Data from the 2003 Experiment

We first compare the data from 2003 with those of 1995 in the frequency domain. To this end, we have computed average power spectra for stations 24 (1995 experiment) and Mo51 (2003 experiment). We computed the power spectra for each of the one-minute windows taken from the data, and averaged them geometrically for each of those two stations. A total of 134 one-minute windows could be averaged for station P24, and a total of 126 for station Mo51. We have not corrected for instrument response, and each of the averaged power-spectral densities had to be multiplied by an arbitrary factor to be able to compare them with the Peterson (1993) global high and low noise models. This comparison is shown in Figure 10. For frequencies above 2 Hz, there is no significant difference between the 40 sec and the 1 Hz seismometers. For lower frequencies, the 1 Hz sensor clearly

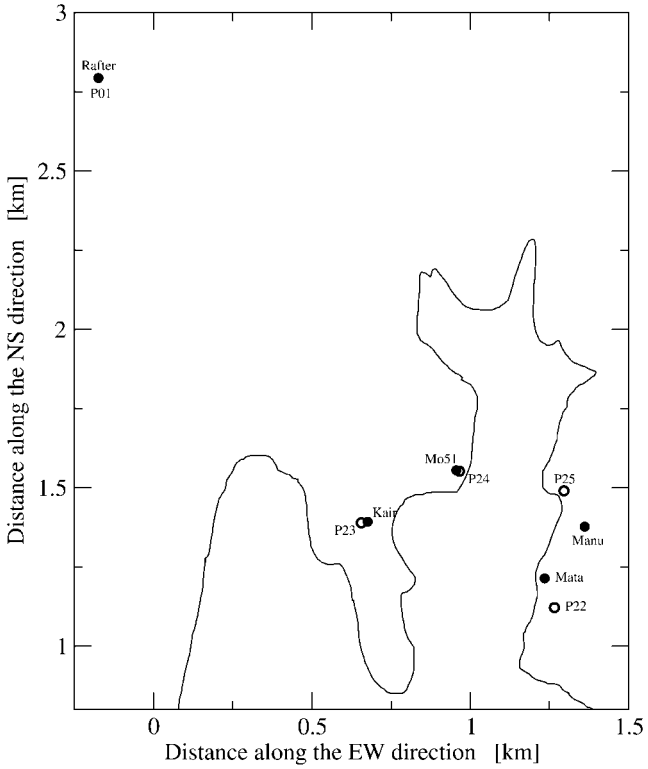

Figure 9. Station distribution of the 2003 experiment. Rock sites used during the 1995 experiment, open circles; Rock sites used during the 2003 experiment, solid circles. Rafter and P01 are located at exactly the same site, as are P24 and Mo51.

attenuates ground motion, relative to the Guralp sensor, which reproduces fairly well the shape of the reference noise curves down to 0.1 Hz. Figure 10 shows that, if the low-frequency resolution of the sensors used in 1995 affected adversely our measurements for frequencies smaller than 1 Hz, we can expect to bring this limit down to at least 0.1 Hz using the data from the Guralp sensors.

An example of the results is shown in Figure 11. This figure shows the crosscorrelation coefficients for two different station pairs, at distances 587 m (for Kair-Mata) and 2088 m (for Manu-Rafter). In the first case, the first zero crossing is at a frequency of about 1.6 Hz, while in the second it is at about 0.6 Hz. Thus, we can conclude that the lack of correlation observed among the rock stations using data from the 1995 experiment was due to the low-frequency limitation of the sensors, which could not correctly record ground motion at 0.6 Hz.

It is possible to make an additional observation, comparing the frequency of the first zero for Kair-Mata with those shown in Figure 3. This frequency is 1.6 Hz for a distance of 587 m in Figure 11, while it is 1.2 Hz for distances around 300–400 m in Figure 3a. Our interpretation is that the argument of the Bessel function (and therefore the abscissa of its first zero crossing) depends both on distance between stations and on phase velocity. A different phase velocity will change the value of the argument, even if the distance between stations remains fixed. This is shown in Figure 12, where we have plotted the same data shown in Figure 3a, but adding now the points obtained during the 2003 experiment, and the points obtained from the rock stations of the 1995 experiment, for which the frequency of the first zero crossing could be determined. We mentioned earlier that these frequencies were inconsistent between the sediment and the rock stations. Figure 12 shows that they are very consistent between the rock stations operated in 1995 with those operated in 2003. The subsoil structure, as observed through the correlation between ambient vibration measurements at two stations, is not the same between stations on the sediments and stations on rock. In order to obtain a result using SPAC, we need significant correlation between two stations. This requirement is not satisfied for two stations where one is on sediments and one on rock. It is satisfied if the two stations are on rock, although the results were adequate only for 4 station pairs (24–25, 22–25, 22–24, and 22–23) from the 10 possible rock station pairs in 1995. Figure 12 also shows that we get significant correlation between the rock stations close to the valley and station Rafter, at distances larger than 1.6 km, even if the soil conditions differ. The wavelengths which are correlated at these large inter-station spacings must be guided by the subsoil stratigraphy that is common between rock stations close to Parkway valley and Rafter.

The correlation coefficients from the 2003 experiment were inverted to estimate the phase-velocity dispersion curve with the same procedure used for the data from 1995. The values used for the parameters of the *a priori* model were the same as in the case of the 1995 data. Again, we repeated several times the inversion procedure, using different values to verify that their choice (within reasonable limits) did not have a significant impact on the final solution. The results are shown in Figure 13 with solid circles. We observe that the correlation coefficients computed at larger inter-station distances allows us to obtain phase velocities for frequencies as low as 0.4 Hz. The phase-velocity values are quite large, around 3 km/s in the range 0.5–1 Hz. This value corresponds to wavelengths between 3 and 6 km. For these long waves, ground motion, guided by deep layers, is correlated between the stations immediatly outside Parkway basin (on the weathered greywacke) and Rafter, on firm rock. The open circles in Figure 13 show the phase velocity values determined from the 1995 data. The phase velocities from the two experiments show a good agreement for frequencies larger than 1.5 Hz. However, according to Henstridge's (1979) criterion, the results from 2003 are not reliable for frequencies larger than 1.4 Hz. We confirm then that the results using the SPAC method and the data from 1995 are not correct for frequencies around the resonant frequency of the basin (between 1.5 and 2 Hz; Chávez-García *et al.*, 1999). Figure 13 also shows the phase-velocity estimates obtained using *f–k* analysis for the ten best recorded seismic events at Parkway (open diamonds in Figure 13; Chávez-

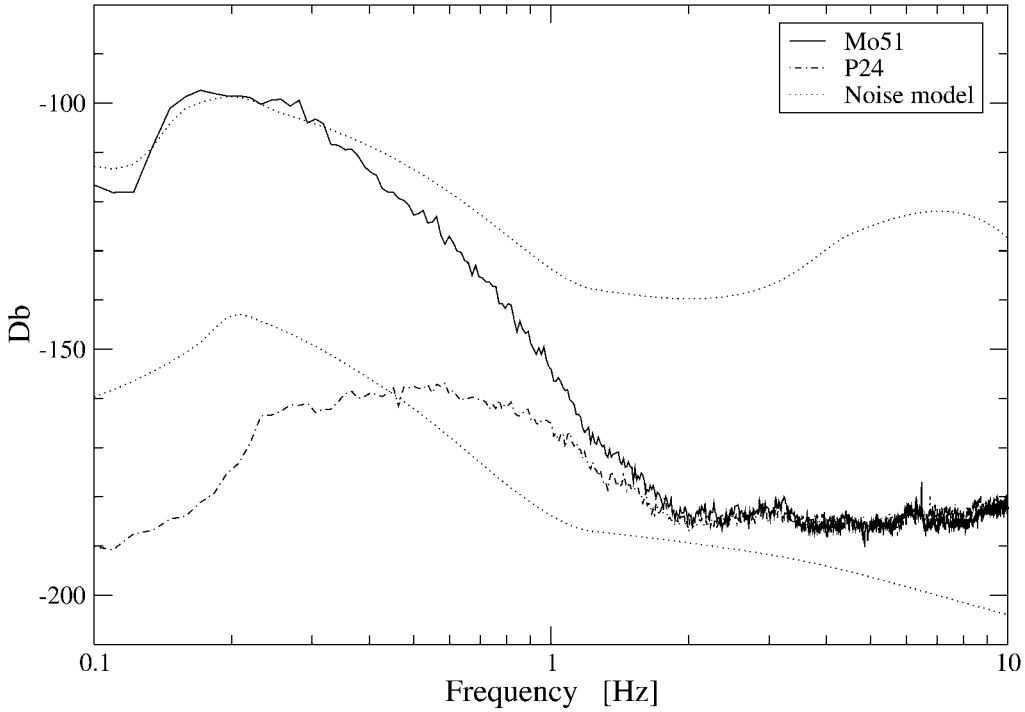

Figure 10. Geometric average of the Fourier power spectra of noise measurements observed at station P24 (1995 experiment, dot-dashed line) and at station Mo51 (2003 experiment, solid line). These curves result from the averaging of 134 (P24) or 126 (Mo51) individual spectra computed for one-minute windows. The dotted lines show the Peterson (1993) global high and low noise models. Zero dB corresponds to an amplitude of 1 (m/sec)2/Hz. The amplitude of observed power spectra densities was affected by an arbitrary amplitude factor, as we have not corrected for instrument response.

García, 2002). Finally, we also compare the estimates of phase velocity with the dispersion curve computed for the fundamental mode for the startigraphy determined at Parkway by Stephenson and Barker (2000) using seismic CPT. The shear-wave velocity of the basement, in the model by Stephenson and Barker (2000), is 1.75 km/sec. The phase velocity estimated from the 2003 experiment suggests that the halfspace shear-wave velocity is much larger. Our results from SPAC do not give indications of a layer with an *S*-wave velocity of 1.75 km/sec, from neither of the two experiments. This suggests that our results are lacking an intermediate scale that would bridge the gap between the phase velocity determined for the sediments filling Parkway basin, and the 3 km/sec for some deep basement common to Rafter and the weathered greywacke. A possible explanation could be that the 3 km/sec correspond to unweathered bedrock, while the SCPT stopped at the weathered greywacke, of 1.75 km/sec shear-wave velocity. A large distance interval for which we do not have measurements is shown in Figure 12, between 0.7 and 1.6 km.

Our results from the 1995 and 2003 experiments seem to have left uncovered a range of frequencies in the phase-velocity dispersion curve determined for Parkway. In this gap would be the shear-wave velocity of the weathered greywacke, around 1.75 km/sec according to Stephenson and Barker (2000). Yu and Haines (2003) computed the site amplification at Parkway using spectral ratios for the earthquake data recorded in 1995. They evaluated the suitability of the station on the weathered greywacke as reference station relative to station P01 (colocated with Rafter). They showed that the amplification level and the resonant frequency computed at the soft soil stations was independent of the reference station used. They also showed that the stations on the greywacke did not amplify ground motion, relative to station P01. The 1D amplification that can be readily computed from the profile given by Stephenson and Barker (2000) is a factor of 12.4 (neglecting attenuation), very similar to the maximum observed in spectral ratios of recorded earthquake motion (a factor of 12 for station 10, EW component, relative to station 25). Therefore, we may infer that there is no large impedance contrast in the layers below the sediments in Parkway basin, and that subsoil structure probably consists of a velocity gradient between 1.75 km/sec, just below the sediments, down to 3 km/sec at several km depth.

Conclusions

In this article we have presented a different view of the standard SPAC method of analysing microtremor records.

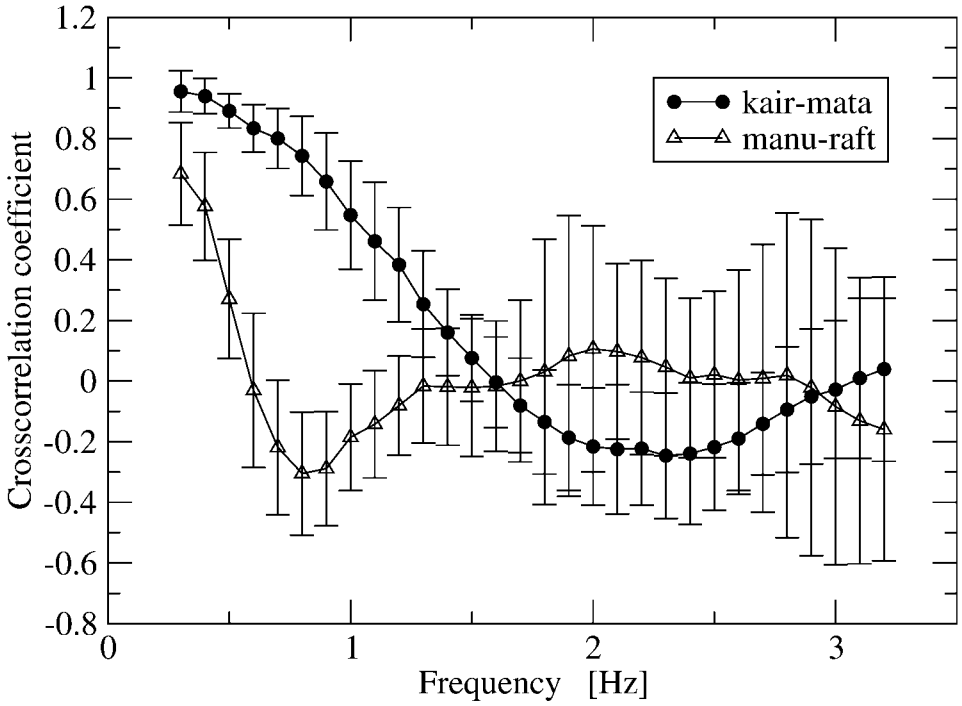

Figure 11. Examples of crosscorrelation coefficients computed for two different station pairs, using data from the 2003 experiment. The names of the stations correspond to those given in Figure 9. Distance between stations is 587 m for Kair-Mata, and 2088 m for Manu-Rafter.

We have shown that it is possible to exchange duration of the records for the spatial averaging required by the method. The possibilities that this result opens are large, because it is not often possible to install the stations in the precise circular geometry required by SPAC (in an urban situation it becomes clearly impossible). However, if we are able to record microtremors for a long enough time, and the ambient vibration wavefield is stationary in time and space, we can substitute temporal average instead of the azimuthal average required by SPAC. However, this is valid only if the sources of ambient vibration or the subsoil structure do not impose a predominant direction of propagation, as is the case in Parkway valley. This allowed us to compute average crosscorrelation coefficients for many different distances using our datasets, as opposed with standard studies that use SPAC, where only two or three different distances are the norm.

In the case of Parkway basin, we have shown that using our interpretation of SPAC it is possible to obtain a phase-velocity dispersion curve that is in good agreement with independent results. Ambient vibration within the valley is not correlated with that recorded by stations on rock nearby. The stations on the soft sediments allow the sediment velocity to be constrained and indicate that a large impedance contrast exists at the base. They are unable, however, to determine the velocity of the substratum. The use of a different dataset, recorded eight years later and using broadband seismometers, allowed us to show that the limitations of the 1995 dataset came from the instruments. The data of the 2003 experiment showed that the microtremor wavefield is correlated at distances larger than 2 km. SPAC, as with all other array analysis methods, requires lateral uniformity of the subsoil structure for all stations composing the array. The necessary lateral uniformity, however, is a function of wavelength.

The phase-velocity dispersion curve obtained from our analysis is in very good agreement with previous estimates at Parkway. This suggests that the vertical components of microtremor recordings are dominated by Rayleigh waves, propagating with uniform power in many different directions. We observe, however, that we could not constrain the phase velocity of the layers going from the weathered greywacke, just below the sediments at Parkway and with a shear-wave velocity of 1.75 km/sec (Stephenson and Barker, 2000), to a deep layer with shear-wave velocity around 3 km/sec. The spectral ratio computations by Yu and Haines (2003) indicate, however, that there is no strong velocity discontinuity in these layers.

Acknowledgments

The careful reviews by A. M. Dainty and two anonymous reviewers allowed us to improve greatly the presentation. The operation of the Parkway network was supported by the New Zealand Foundation for Science, Research and Technology, under Contract C05620. This research was partially supported by CONACYT, Mexico, under contract 32588-T and by DGAPA, UNAM, under contract IN104800.

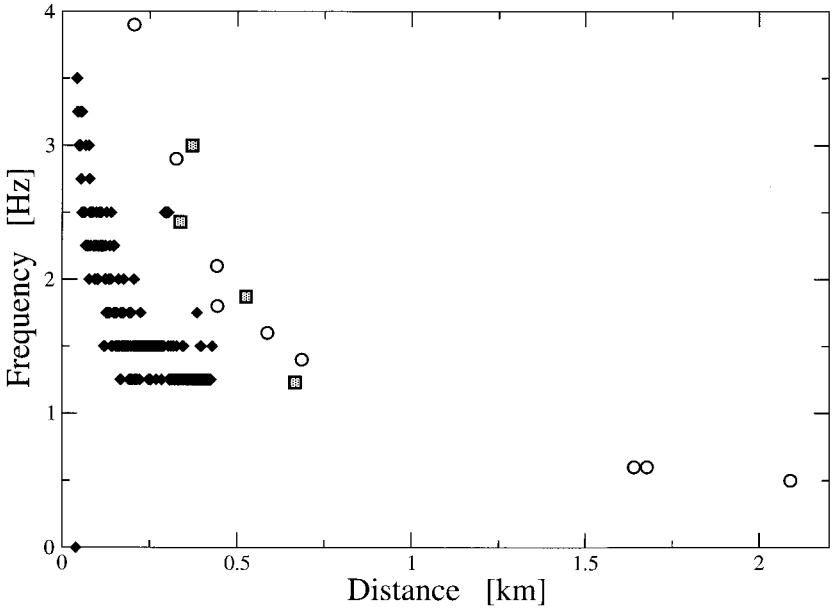

Figure 12. Frequency of the first zero crossing of the correlation coefficients (average values) as a function of inter-station distance. Results for the stations on the sediments using data from the 1995 experiment (same data points shown with solid diamonds in Figure 3a), solid diamonds; results for four pairs of stations on rock using data from the 1995 experiment, dotted squares; results using data from the 2003 experiment, open circles.

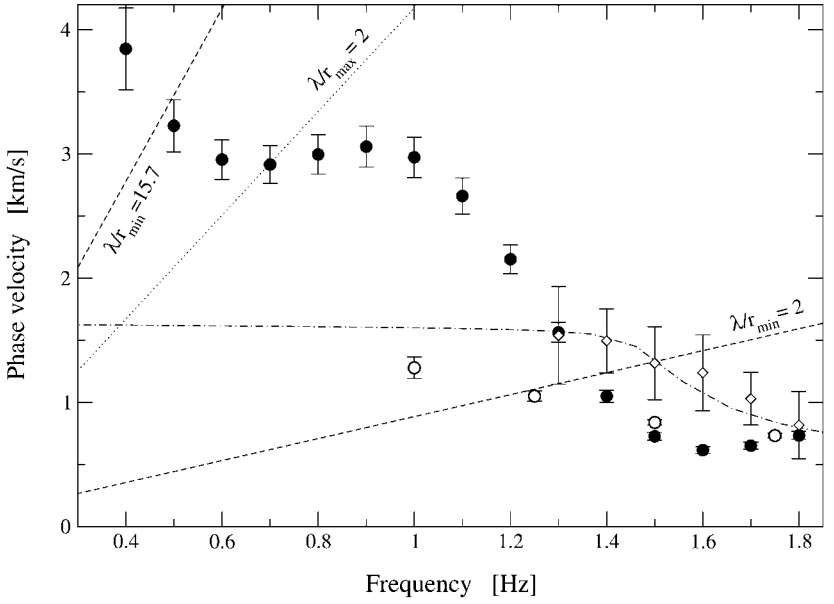

Figure 13. Phase-velocity dispersion curve inverted from the correlation coefficients computed using the data from the 2003 experiment, solid circles. The dotted and dashed lines show the limits imposed by Henstridge's (1979) criterion, computed for $r_{max} = 2088.4$ m and $r_{min} = 442$ m. λ is the wavelength. The open circles show, for comparison the phase velocity values obtained using the data from the 1995 experiment (solid circles in Figure 8). The open diamonds show the phase velocity obtained from the detailed *f–k* analysis of earthquake data recorded by Parkway array for the 10 best recorded events (Chávez-García *et al.*, 2002). The dot-dashed line shows the fundamental mode phase-velocity dispersion curve computed for the model established by Stephenson and Barker (2000) for Parkway basin.

References

Aki, K. (1957). Space and time spectra of stationary stochastic waves, with special reference to microtremors, Tokyo University, *Bull. Earthquake Res. Inst.* **25,** 415–457.

Aki, K. (1965). A note on the use of microseisms in determining the shallow structure of the earth's crust, *Geophysics* **30,** 665–666.

Aki, K., and P. G. Richards (1980). *Quantitative Seismology*, W. H. Freeman, New York.

Asten, M. W. (1976). The use of microseisms in geophysical exploration, *Ph.D. Thesis*, Macquarie University.

Asten, M. W. (1978). Geological control on the three-component spectra of Rayleigh wave microseisms, *Bull. Seism. Soc. Am.* **68,** 1623–1635.

Barker, T. (1988). Array processing of Rayleigh waves for shallow shear-wave velocity structure, *Seism. Res. Lett.* **59,** 12.

Bettig, B., P. Y. Bard, F. Scherbaum, J. Riepl, F. Cotton, C. Cornou, and D. Hatzfeld (2001). Analysis of dense array noise measurements using the modified spatial auto-correlation method (SPAC): application to the Grenoble area, *Boll. Geof. Teor. Appl.* **42,** 281–304.

Capon, J. (1969). High-resolution frequency-wavenumber spectrum analysis, *Proc. IEEE* **57,** 1408–1418.

Capon, J., R. J. Greenfield, R. J. Koller, and R. T. Lacoss (1968). Short-period signal processing results for the large aperture seismic array, *Geophysics* **33,** 452–472.

Chávez-García, F. J., G. Pedotti, D. Hatzfeld, and P. Y. Bard (1990). An experimental study of site effects near Thessaloniki (Northern Greece), *Bull. Seism. Soc. Am.* **80,** 784–806.

Chávez-García, F. J., W. R. Stephenson, and M. Rodríguez (1999). Lateral propagation effects observed at Parkway, New Zealand: A case history to compare 1D versus 2D site effects, *Bull. Seism. Soc. Am.* **89,** 718–732.

Chávez-García, F. J., J. Castillo, and W. R. Stephenson (2002). 3D site effects: A thorough analysis of a high quality dataset, *Bull. Seism. Soc. Am.* **92,** 1941–1951.

Chouet, B. C., G. DeLuca, P. Milana, M. Dawson, C. Martín, and R. Scarpa (1998). Shallow velocity structure of Stromboli volcano, Italy, derived from small-aperture array measurements of Strombolian tremor, *Bull. Seism. Soc. Am.* **88,** 653–666.

DeLuca, G., R. Scarpa, E. Del Pezzo, and M. Simini (1997). Shallow structure of Mt. Vesuvius volcano, Italy, from seismic array analysis, *Geophys. Res. Lett.* **24,** 481–484.

Dziewonski, A. M., S. Bloch, and M. Landisman (1969). A technique for the analysis of transient seismic signals, *Bull. Seism. Soc. Am.* **59,** 427–444.

Ferrazzini, V., K. Aki, and B. Chouet (1991). Characteristics of seismic waves composing Hawaiian volcanic tremor and gas-piston events observed by a near-source array, *J. Geophys. Res.* **96,** 6199–6209.

Gledhill, K. R., M. J. Randall, and M. Chadwick (1991). The EARSS digital seismograph: system description and field trials, *Bull. Seism. Soc. Am.* **81,** 1380–1390.

Henstridge, D. J. (1979). A signal-processing method for circular arrays, *Geophysics* **44,** 179–184.

Herrmann, R. B. (1973). Some aspects of band-pass filtering of surface waves, *Bull. Seism. Soc. Am.* **63,** 663–671.

Herrmann, R. B. (1987). *Computer Programs in Seismology*, S. Louis University, 7 vols.

Kanno, T., K. Kudo, M. Takahashi, T. Sasatani, S. Ling, S. S., and H. Okada (2000). Spatial evaluation of site effects in Ashigara valley based on *S*-wave velocity structures determined by array observations of microtremors, in *Proc. 12th World Conf. on Earthq. Eng.*, Auckland, New Zealand, 30 January–4 February 2000. [New Zealand Society for Earthquake Engineering, CD-ROM.

Lacoss, R. T., E. J. Kelly, and M. N. Toksoz (1969). Estimation of seismic noise structure using arrays, *Geophysics* **34,** 21–38.

McMechan, G. A., and M. J. Yedlin (1981). Analysis of dispersive waves by wave-field transformation, *Geophysics* **46,** 869–874.

Menke, W. (1984). *Geophysical Data Analysis: Discrete Inverse Theory*, Academic Press, 260 pp.

Metaxian, J. P. (1994). Etude sismologique et gravimétrique d'un volcan actif: Dynamisme interne et structure de la Caldeira Masaya, Nicaragua, *Ph.D. Thesis*, Université de Savoie, 319 pp. (in French).

Morikawa, H., K. Toki, S. Sawada, J. Akamatsu, K. Miyakoshi, J. Ejiri, and D. Nakajima (1998). Detection of dispersion curves from microseisms observed at two sites, in The effects of surface geology on seismic motion; Proc. of the 2nd. Intl. Symp. on the effects of surface geology on seismic motion, K. Irikura, K. Kudo, H. Okada, and T. Sasatani (Editors) **2,** 719–724.

Nazarian, S., and K. H. Stokoe, II (1984). In situ shear-wave velocities from spectral analysis of surface waves, in *Proc. of the 8th World Conf. on Earthq. Eng.* **8,** 21–28.

Ohori, M., A. Nobata, and K. Wakamatsu (2002). A comparison of ESAC and FK methods of estimating phase velocity using arbitrarily shaped microtremor arrays, *Bull. Seism. Soc. Am.* **92,** 2323–2332.

Papoulis, A. (1984). Probability, Random Variables, and Stochastic Processes, McGraw-Hill, Singapore, 576 pp.

Peterson, J. (1993). Observation and modeling of seismic background noise, *U.S. Geol. Surv. Open-File Rep. 93-332*.

Scherbaum, F., J. Riepl, B. Bettig, M. Ohrnberger, F. Cotton, and P. Y. Bard (1999). Dense array measurements of ambient vibrations in the Grenoble basin to study local site effects, AGU.

Stephenson, W. R., and P. R. Barker (2000). Seismic CPT in strong soils, Earthquake Commission Research Project 99/380, Client Report 2000/47, Institute of Geological and Nuclear Sciences, Lower Hutt, New Zealand.

Tarantola, A., and B. Valette (1982). Generalized nonlinear inverse problems solved using the least squares criterion, *Rev. Geophys. Space Phys.* **20,** 219–232.

Toksoz, M. N. (1964). Microseisms and an attempted application to exploration, *Geophysics* **24,** 154–177.

Yamamoto, H. (1998). An experiment for estimating *S*-wave velocity structure from phase velocities of Love and Rayleigh waves in microtremors, in The effects of surface geology on seismic motion; Proc. of the 2nd. Intl. Symp. on the Effects of Surface Geology on Seismic Motion, K. Irikura, K. Kudo, H. Okada, and T. Sasatani (Editors), Rotterdam, Balkema, **2,** 705–710.

Yu, J., and J. Haines (2003). The choice of references sites for seismic ground amplification analyses: case study at Parkway, New Zealand, *Bull. Seism. Soc. Am.* **93,** 713–723.

Instituto de Ingeniería, UNAM, Apdo. Postal
70-472, Coyoacán, 04510 México, D.F.
Mexico
(F.J.C.-G., M.R.)

Institute of Geological and Nuclear Sciences,
Ltd., Gracefield Road, P.O. Box 30 368, Lower
Hutt, New Zealand
(W.R.S.)

Manuscript received 29 August 2003.